

# A high concentration rooftop photovoltaic system

Philip Gleckman

Energy Innovations, Inc., 130 West Union St., Pasadena, CA, USA 91103

## ABSTRACT

The commercial rooftop environment poses difficult challenges for concentrating photovoltaic (CPV) systems. Rooftop CPV must not only meet low cost and high energy production targets common to ground mounted systems but also must solve safety, wind loading, and area usage requirements in ways that are compatible with the rooftop environment. To meet these requirements we have developed a low-profile carousel-mounted array of Fresnel concentrators using triple junction solar cells. In this paper we describe the key features of the opto-mechanical and thermal design for manufacturability and reliability. These features include the concentration level, the mechanical drive scheme, the configuration of the lens with secondary optical element, and passive cooling. Also described are elements of the optical component testing and assembly methods. We present exemplary results of environmental testing and measurements of electro-optical performance.

**Keywords:** Concentrating, photovoltaic, Fresnel, secondary, carousel

## 1. INTRODUCTION

Energy Innovations, through its system integration arm EI Solutions, has installed several megawatts of grid-tied flat-plate photovoltaic power to commercial and government customers. This PV engineering and finance experience has been instrumental in the development of our concentrator product by guiding the design to meet the challenging performance and cost requirements of the commercial rooftop.

In this paper we describe the key system requirements and how we achieved them in the Sunflower<sup>TM</sup> product's high concentration opto-mechanical architecture. High concentration leads to sensitive assembly and tracking; we present quantitative examples of the tolerances in our design and practical approaches to accommodate them. As there is little heritage in concentrator products we are faced with many new reliability issues. We give an analysis of some of the reliability issues that specifically relate to the optical components and materials.

## 2. SYSTEM REQUIREMENTS

To be accepted on the commercial rooftop, any PV product needs to meet requirements in several categories including cost/performance, size and weight, ease of installation, simplicity of operation, environmental conditions, safety, and reliability. In order to compete with conventional flat-plate PV the fully installed pre-rebate costs must be less than  $\sim 8$ - $10$   $\$/W_p$  AC.  $W_p$  is the "peak" electrical power measured at so-called PTC conditions of  $900 \text{ Wm}^{-2}$  insolation,  $1 \text{ ms}^{-1}$  wind speed, and  $20^\circ\text{C}$  ambient temperature. A CPV system also needs to compete with flat-plate on an annual energy production basis. As a measure of annual energy production we use the ratio of the first year's AC energy in kWha to  $W_p$  (where  $W_p$  is measured at PTC conditions and the "a" in kWha stands for annual). This "production ratio" is equivalent to the product of capacity factor and the number of hours. To compete with flat-plate PV the production ratio should be at least  $1.5 \text{ kWha}/W_p$ . Production ratio will depend strongly on the location due to weather.

The “area efficiency” (defined as the first year’s energy production per square meter of rooftop) is an important factor on the rooftop with limited space. In principle CPV could have higher area efficiency than flat-plate PV but it is difficult to achieve in practice.

The weight of the heaviest component that is installed on the roof should be less than what two people could reasonably lift. This has constrained the weight of our assembled power unit to be less than 65 kg. Furthermore, when installed, the distributed pressure on the roof should not exceed 190 Pa. Shipping costs control the unit’s size.

A rooftop CPV system should not require monitoring or maintenance (other than elective washing) after initial set up. The system should power itself. Nearly all the units making up the system should commence operating in less than one hour every morning (absent unusual weather conditions) when the sun’s altitude has reached 10°.

For a large market like California the rooftop presents severe environmental requirements. These are summarized in Table 1. In addition to the entries in Table 1 a rooftop product in California needs to withstand seismic activity and loading due to snow accumulation.

Table 1. Rooftop environmental conditions

Condition	Value
Ambient temperature (operating)	0 to 40 °C
Ambient temperature (withstanding)	-20 to 50 °C
Wind (withstand without damage)	53.7 m/s
Hail	25 mm diameter at 25.7 m/s
Humidity	100%

Acceptance by building inspectors and rooftop customers requires that the product meet the safety requirements needed for UL certification.

The reliability of the product can be defined in terms of the number of years it takes for the original rated electrical output of the overall system to degrade to an acceptable level. For example, under the California Solar Initiative a PV system must have a warranty to cover against the rated output falling more than 15% in ten years.

### 3. OPTO-MECHANICAL ARCHITECTURE

#### 3.1 Arrays of power units

We have developed a product architecture that meets the system requirements outlined in the previous section. The architecture hierarchy is as follows. The overall PV system is laid out in a hexagonal array of power units. Each unit produces about 233 W<sub>p</sub> DC at PTC conditions. A unit consists of three linear arrays of Fresnel lenses paired with solar cell receivers. Fig. 1a shows a rendering of the hexagonal array. The aisles between units allow access for maintenance if necessary and are accounted for in area efficiency calculations. Fig. 1b shows an isolated unit that independently tracks the sun with a single azimuth stage (carousel) and three independent altitude axes for each of the three modules. There are four sensors (three for altitude and one for azimuth) per unit which operate in a closed loop control system with the precision required by the small field of view optical system. The small flat-plate solar cell module shown in Fig. 1b is used to power the actuation system.

For this scheme to track the sun adequately the three module rotation axes must be nearly parallel. It can be shown that the relation between pointing error and azimuth error is:

$$\cos \delta = \sin^2 \theta \cos \Delta\phi + \cos^2 \theta$$

where  $\delta$  is the pointing error,  $\theta$  is the zenith angle, and  $\Delta\phi$  is the azimuth error. Unlike the case of altitude, a degree of azimuth error corresponds to less than a degree of pointing error except at zero altitude. Therefore, the annual energy produced is less sensitive to azimuth error than to altitude error.



Fig. 1a. Hexagonal array of power units

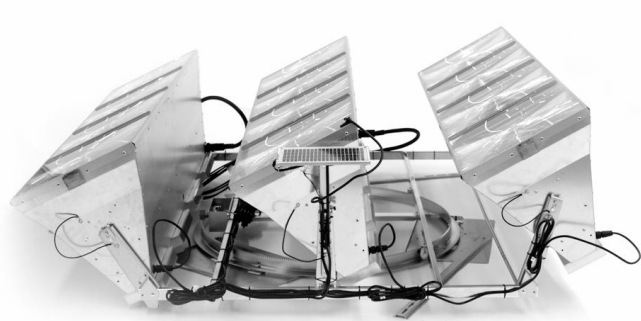


Fig. 1b. Unit with three independent altitude axes and common azimuth stage

### 3.2 Enclosed modules of Fresnel lens concentrators

Each module contains four lenses, secondaries, and solar cell receivers all mounted to sheet metal tub housing. The optical train is depicted in Fig. 2. An inexpensive grooves-in molded plastic Fresnel lens concentrates the sunlight onto a glass secondary optical element which is optically coupled to the TJSC. The lens aperture is  $0.106 \text{ m}^2$  and the cell active area is approximately  $0.88 \text{ cm}^2$ , corresponding to a geometric concentration ratio of  $\sim 1200:1$ . The high efficiency ( $\sim 35\%$ ) of the cell is critical to reducing the CPV system cost of energy relative to flat-plate single crystal silicon (with module efficiency  $\sim 14\%$ ). The high concentration ratio used in the Sunflower<sup>TM</sup> optical architecture enables cost effective use of these efficient cells by producing a high power density and by producing more voltage from the cells at fixed temperature. The open circuit voltage  $V_{oc}$  depends logarithmically on the irradiance at fixed temperature. For  $\text{GaInP}_2\text{-GaAs-Ge}$  cells the open circuit voltage  $V_{oc}$  has a negative temperature coefficient  $\sim -4 \text{ mV}/^\circ\text{C}$  at high concentration. The cell temperature is maintained at  $\sim 70^\circ\text{C}$  at PTC conditions through passive cooling with aluminum heat sinks thermally coupled to the cell substrate.

The tub depth is driven by two opposing demands, *viz.* high lens efficiency and low shipping cost. On-axis, the lens efficiency is primarily determined by Fresnel reflection losses for the outer facets, scattered light from tip rounding and draft, and transverse axial chromatic aberration. Of these only the reflection losses are significantly reduced by higher  $f/\#$ . Comatic aberration, which has an effect on the tracking sensitivity, decreases at higher  $f/\#$ . We achieved a favorable balance between efficiency and shipping cost with the lens designed for  $f/0.84$ . The (solar cell current weighted average) molded lens efficiency is  $\sim 80\%$ .

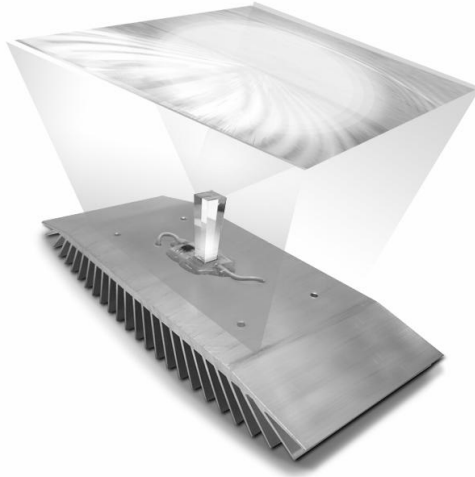


Fig. 2. Concentrator optical train

### 3.3 Secondary optical element

The secondary optical element serves primary to eliminate flux and thermal gradients at the cell in order to maintain high fill factor and voltage. The secondary concentration ratio (ratio of field stop area to cell area) is limited by étendue conservation thus:

$$C_s < \text{PSA}_{\text{cell}} / \text{PSA}_{\text{lens}} \cdot n^2.$$

where  $C_s$  is the secondary concentration ratio, PSA is the projected solid angle of the light incident on the cell or exiting from the lens, and  $n$  is the immersion index of the cell. The PSA of the lens is given by<sup>1</sup>:

$$\text{PSA}_{\text{lens}} = \arctan(\sin\gamma) \cdot \sin\gamma$$

where  $\gamma$  is the semi-angle subtended by the lens edge from the field stop. For the case of a glass secondary  $n \sim 1.5$  and a maximum angle of incidence (AOI) at the cell of  $\sim 50^\circ$  the (square) secondary aperture is less than  $\sim 21$  mm for efficient light transfer to the cell. This field stop dimension limits the tracking sensitivity of the system. For a reflective secondary with  $n = 1$  and AOI  $\sim 80^\circ$  (in air) the corresponding aperture is  $\sim 18$  mm.

### 3.4 Cell AOI sensitivity

As explained above, the maximum AOI at the cell plays a role in determining the secondary design and the tracking sensitivity. Therefore, we measured the response of the cell as a function of AOI in a medium with  $n \sim 1.5$  with the apparatus shown in Fig. 3a. Light from a xenon lamp is focused through a hemisphere of acrylic optically coupled to the cell and the assembly is rotated about the cell while the current is measured. The incident and fainter reflected light can be observed. The relative current is plotted in Fig. 3b. There is very little reduction in current for AOI  $< 50^\circ$ . Overlaid on Fig. 3b is the calculated longitudinally averaged (*i.e.* around the cell normal) intensity. Integrated over the light distribution the relative reflection loss is less than 1% with this secondary design.

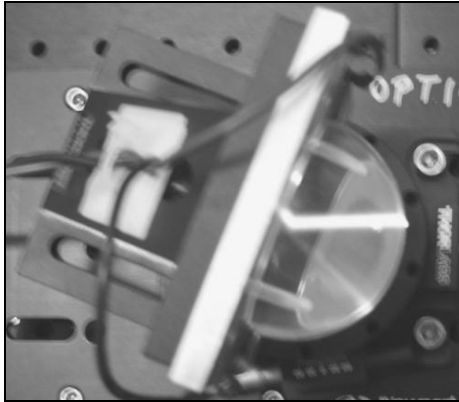


Fig. 3a. AOI sensitivity apparatus

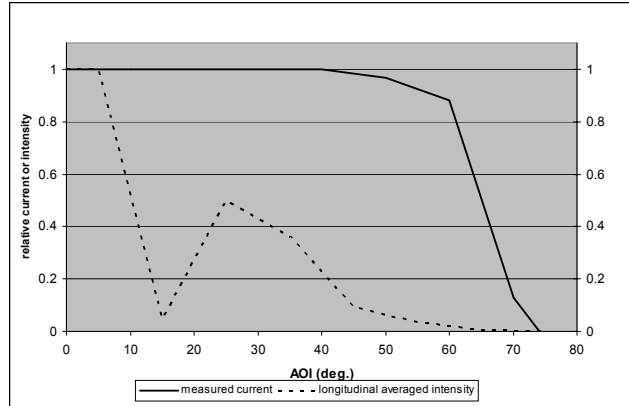


Fig. 3b. AOI response compared with simulated intensity

## 4. ASSEMBLY AND TRACKING TOLERANCES

We have discussed how the system requirements on cost/performance and shipping have influenced the high concentration opto-mechanical design. The sensitivity of the opto-mechanical design to position and alignment errors determines the specifications for assembly and tracking that must be achieved for an acceptable level of performance.

### 4.1 Assembly tolerances

At the unit level, since there is a common azimuth drive for all three modules the mounting system for these modules must provide for a high degree of parallelism of their axes. At the module level it is critical to ensure that the four concentrators are mutually aligned in such a way that the four gut rays (*viz.*, the rays connecting the centers of the cells to the centers of their corresponding lenses) are parallel to an acceptable angle tolerance. Otherwise, there will be a shift in one or more solar images that cannot be compensated by tracking. The sensitivity to image shift (or equivalently receiver decenter) is shown in Fig. 4. The dotted line indicates the tolerance below which there is negligible loss relative to that with no receiver decenter.

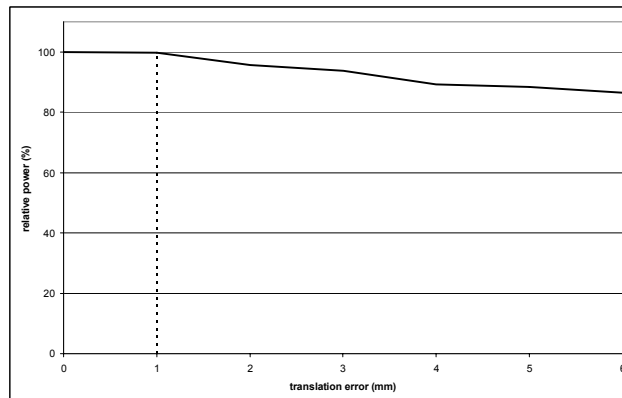


Fig. 4. Measured power loss due to receiver decenter

We have constructed a vision system apparatus for verifying the parallelism of the gut rays from the four concentrators. This is shown schematically in Fig. 5. First, a movable telescope calibrates the alignment of the four video cameras. The telescope is then removed and the module under test is installed. A small amount of current is injected into the solar cells and the cameras measure through the Fresnel lens the displacement of the secondary's image from its theoretical center. The resolution of the Fresnel lens and camera allow the detection of displacement errors  $\ll 0.5$  mm.

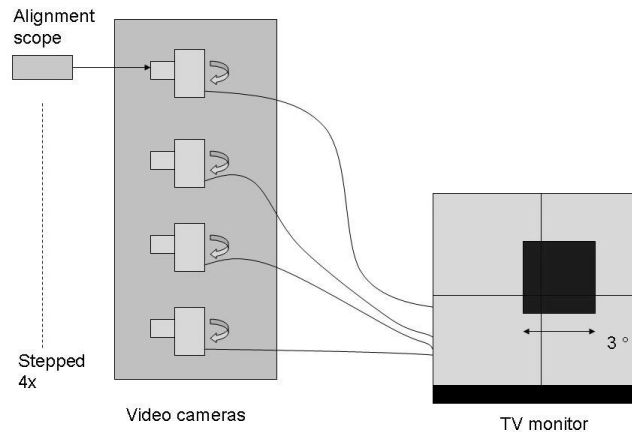


Fig. 5. Alignment verification scheme

At the individual concentrator level there are other tolerances to consider in the mechanical design including lens tilt, secondary tilt, and lens-receiver airspace, but power is less sensitive to these degrees of freedom.

## 4.2 Tracking sensitivity

To first order, imperfect tracking of the sun causes a translation of the solar image at the field stop. This effect was characterized in section 4.1. A second order effect due to tracking error is a change in the shape of the irradiance distribution due to off-axis aberrations. Measurements were made of the tracking sensitivity by allowing the solar image to traverse the secondary aperture while measuring maximum power and circuit current  $I_{sc}$ . The results are shown in Fig. 6 for the case of a reflective secondary and compared with a simulation. The fact that the power and current curves are nearly the same implies that fill factor reduction due to a reduction in off-tracked uniformity is not significant. The  $I_{sc}$  simulation calculates the minimum carrier generation of the junctions for each solar position. The simulation slightly overestimates the current for sun AOI  $< 1^\circ$ . The measurements indicate a relative drop of 50% at  $1.25^\circ$  and 5% at  $0.35^\circ$ . This should be compared to what is achievable by the tracking system.

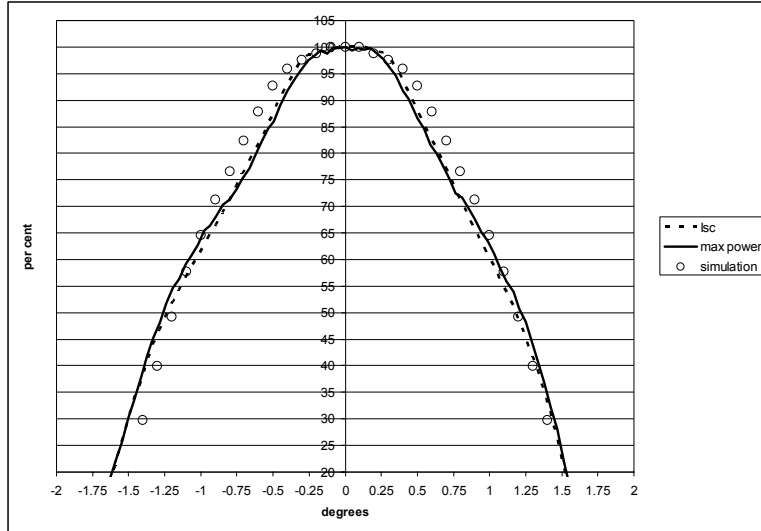


Fig. 6. Measured and simulated relative tracking loss

An exemplary measurement using an auxiliary sensor of the tracking error as a function of time for the module altitude is shown in Fig. 7. You can see that when the sun has moved by  $1/20^\circ$  the mechanical system issues a correction to restore alignment. An error of  $1/20^\circ$  does not degrade the power at all, as can be seen in Fig. 6.

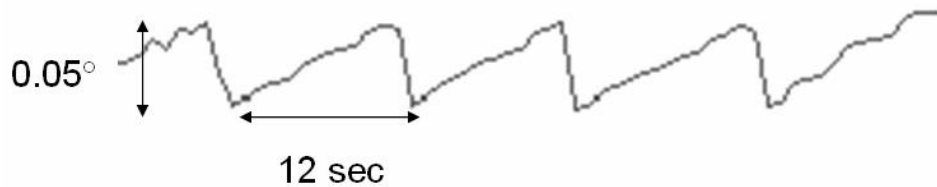


Fig. 7. Measured altitude tracking error

## 5. RELIABILITY OF THE OPTICAL COMPONENTS

In addition to the reliability of the mechanical system (*e.g.* motors and gear boxes) the optical components and materials must be shown to be reliable, primarily the optical adhesive used to bond a glass secondary to the cell, the glass secondary itself, and the Fresnel lens.

## 5.1 Optical adhesive

The optical adhesive is used to minimize reflection losses between the glass secondary and the cell. It must maintain high clarity and adequate adhesion while being subjected to high flux of ultraviolet radiation for fifteen years or more. The simulated spectral distribution delivered by the glass secondary is shown in Fig. 9. The simulation assumes a standard incident AM1.5 direct solar spectrum<sup>2</sup>. The spectrum is divided into three regions: UVA, UVB, and UVV.

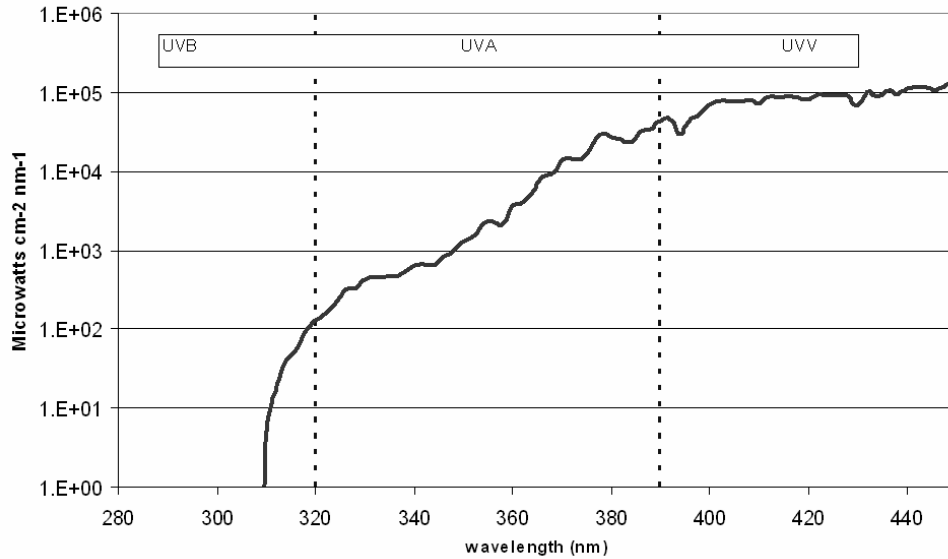


Fig. 9. Spectral power distribution at cell

We performed accelerated lifetime testing of various adhesives with short arc mercury lamps. To determine the acceleration factors due to dosage we measured the lamp irradiance in each ultraviolet spectral band and compared it to the calculated annual average cell irradiance for San Diego derived from Fig. 9. The results are summarized in Table 2. Our preferred adhesive has not degraded after substantially more than fifteen years of equivalent UVA and UVB. It is expected that UVV is the least harmful to the adhesive since there is very little absorption in that band.

Table 2. Acceleration factors achievable with the short arc mercury lamp

	UVV	UVA	UVB
Annual average $W\ cm^{-2}$	0.88	0.11	$7 \cdot 10^{-5}$
Xenon lamp $W\ cm^{-2}$	1.3	4.0	0.8
Acceleration factor	1.5	36	11,000
15 yr. equivalent dosage	~ 10 years	~ 5 months	12 hours

## 5.2 Prism

In fifteen years some amount of dust will accumulate on the surface of a glass secondary, and as the glass is disposed near the solar image there is a risk of thermal fracture if the glass type is not chosen properly. Of the various constituents of Arizona Test Dust ferric oxide is the strongest absorber of sunlight. It is present in the amount of 2-5% by weight<sup>3</sup>. To test the resistance to fracture, we uniformly dispersed pure 1  $\mu\text{m}$  ferric oxide particles on secondaries bonded to cells. We were able to find a threshold dust concentration that caused fracture in glass A but no amount of dust would cause fracture in glass B. Photographs taken of these two secondaries after testing are shown in Fig. 10a and 10b. Glass B has a lower Young's modulus and a lower coefficient of thermal expansion than glass A.



Fig. 10a. Glass type A fractured

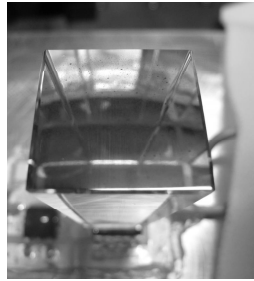


Fig. 10b. Glass type B unharmed

## 5.3 Lens

Three of the most important durability issues for a rooftop Fresnel lens are hail resistance, weatherability, and maintenance of flatness. In order to predict the sensitivity to substrate curvature we simulated the deformation of the lens with the constraint that the orientation of the facets to the substrate was unchanged. For the case of a spherical deformation the simulated relative current produced is plotted as a function of sagitta in Fig. 11. We required that any permanent deformation, which may be due to thermal or moisture induced stress, not exceed 0.5 mm.

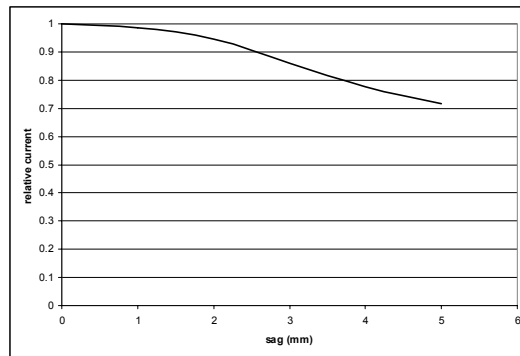


Fig. 11 Simulated deformation loss

We were able to pass the ASTM E1038-98 hail test for photovoltaic modules by choosing a suitable lens material and thickness. The primary weathering factors that degrade the optical (yellowing and haze) and mechanical properties of plastic materials are ultraviolet radiation, heat, and moisture. There are several test protocols available for the assessment of a material under consideration. Among these, there are two that can be carried out in the laboratory environment:

ASTM G 154-06 specifies standard practice for fluorescent lighting, and ASTM G 155-05 specifies the practice for a xenon arc. Both of these standards allow a choice of exposure cycle conditions involving irradiance level, heating, and moisture.

## **6. CONCLUSIONS**

Energy Innovations has developed a high concentration photovoltaic system that meets the system requirements for acceptability on the commercial rooftop. The cost/performance, size and weight, and ease of installation requirements have been achieved through an optimized opto-mechanical architecture that leverages the enabling technology – the TJSC. Any high concentration architecture creates a challenge for assembly and tracking. We have given examples of the sensitivities of our design to assembly and tracking errors, and described practical solutions. There is very little heritage to demonstrate the reliability of concentrator systems. We have described in detail the key reliability challenges regarding the optical portion of the product and some of the testing and analysis we have performed to demonstrate that the product will perform reliably for fifteen to twenty years.

## **ACKNOWLEDGMENTS**

The author would like to acknowledge the contribution of his colleagues at Energy Innovations and EI Solutions towards making the Sunflower™ product successful. The author would also like to thank Steve Chadima and Bill Gross for encouraging him to write this paper.

## **REFERENCES**

1. P. Moon and D. Spencer, *The Photic Field*, The MIT Press, 1981.
2. ASTM G 173-03.
3. ISO 12103-1